

Contribution from the Institute of Molecular Physics, Polish Academy of Sciences, 60-179 Poznań, Poland, and Ecole Nationale Supérieure de Chimie de Paris, CNRS, UA 403, 75231 Paris Cedex 05, France

Electronic and Spectral Properties of Organometallic Tetracyano-*p*-quinodimethane (TCNQ) Salts with Metallocene Stacks

W. Pukacki,^{††} M. Pawlak,[†] A. Graja,[†] M. Lequan,^{*§} and R. M. Lequan[§]

Received July 17, 1986

The two salts $[(\eta^5\text{-C}_5\text{H}_5)\text{Fe}^{\text{II}}\text{Ar}]^+(\text{TCNQ})_2^-$ (Ar = 2,4,6- $\text{C}_6\text{H}_3\text{Me}_3$, C_6Me_6) have been synthesized and characterized by dc conductivity, thermoelectric power, and IR spectroscopy measurements. A quasi-semiconducting behavior of conductivity with temperature-dependent activation energy has been revealed for both salts. A splitting of the 835- cm^{-1} band of the out-of-plane vibration region (880-800 cm^{-1}) of the TCNQ molecule has been found. Observed phenomena have been explained by nonregular charge distribution along the TCNQ chain.

Introduction

During the last 25 years, several organic charge-transfer and inorganic coordination complexes that exhibit high, nearly metallic conductivity have been discovered.¹⁻⁵ The electrical, optical, and other physical properties of these materials are highly anisotropic. It is particularly intriguing to find whether these properties are the manifestation of extended electronic interactions and strong electron-phonon coupling in these materials.

We will consider, here, the physical properties of electrically conducting organometallic TCNQ salts with unprecedented metallocene stacks. The essential feature of these compounds is the presence of one-dimensional segregated stacks of organometallic cations and TCNQ anions.⁶

It is not yet understood how various types of interactions, and hence the physical properties, are affected by the nature of the cations. Such a question can be answered by comparing the physical properties of various TCNQ salts with differently structured and active counterions.

There are many similarities among the highly conducting molecular metals. These materials typically contain parallel segregated chains of large planar molecules. For example, the highly conducting compound based on the donor TTF (tetra-thiafulvalene) and the acceptor TCNQ consists of parallel stacks of TTF^+ and of TCNQ^- . Many of these compounds have the molecules uniformly spaced along the stacks. In the one-electron picture their conduction band is partially filled, thus suggesting their metallic character.

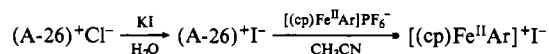
As opposed to the highly conducting materials, the semiconducting TCNQ salts typically contain quasi-linear stacked chains of acceptor ions only. The charge transport properties can be discussed in terms of a one-electron semiconductor model, sometimes with temperature-dependent activation energy or with low-temperature behavior controlled by electrically active impurities.

Because of the unique, three-dimensional molecular structure of metallocene ions, the study of the physical properties of the TCNQ-metallocene complex salts should answer the question about the role of the molecular ordering and the intermolecular interactions in the organic CT (charge-transfer) complexes. Such a question can be answered by the comparison of different organometallic salts. We have therefore synthesized a series of the complexes in which one of the two parallel planar ligands of the metallocene molecules have been varied.

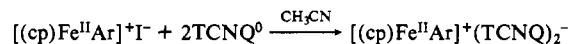
Sample Preparation and Experimental Techniques

The metallocenes of iron in which a metal is complexed by two cyclopentadienyls (cp; $\eta^5\text{-C}_5\text{H}_5$) can form ion-radical salts with organic electron acceptors, e.g. tetracyano-*p*-quinodimethane (TCNQ). Ferrocenes, as well as some of their derivatives substituted at the cyclopentadienyl ring, produce TCNQ compounds with a variety of interesting properties.⁷

As opposed to the above, metallocenes with mixed sandwich cations $[(\text{cp})\text{Fe}^{\text{II}}\text{Ar}]^+$ are not the subject of charge transfer. Thus, we synthesized the ion-radical salts by redox reactions between $[(\text{cp})\text{Fe}^{\text{II}}\text{Ar}]^+\text{I}^-$ and TCNQ. High-purity complexes $[(\text{cp})\text{Fe}^{\text{II}}\text{Ar}]^+\text{I}^-$ were prepared from the parent hexafluorophosphate salts by the exchange with KI on Amberlyst A-26 resin in acetonitrile:



where cp = cyclopentadienyl and Ar = 2,4,6- $\text{C}_6\text{H}_3\text{Me}_3$ (for salt a) or C_6Me_6 (for salt b). The readily prepared metallocene iodides reacted with TCNQ in boiling acetonitrile. The needle- or plate-shaped crystals of the complex salts $[(\text{cp})\text{Fe}^{\text{II}}\text{Ar}]^+(\text{TCNQ})_2^-$ were obtained by slow cooling of the solution:



The salts are stable. The crystal structures of both salts a and b are composed of one-dimensional segregated stacks of organometallic cations and $\text{TCNQ}^{0.5-}$ anions.⁶ The spacings between the central TCNQ rings are uniform; the metallocenes are located on sites of *m* symmetry with the successive cyclopentadienyl and hexamethylbenzene rings on top of each other.

The dc electrical conductivity along the needle axis of the single crystals was measured by the standard four-probe technique. The small size of the crystals, their fragility, and susceptibility to damage on thermal cycling required the utmost precision. For the electrodes, 30- μm silver wires were used; electrical contacts were assured by wetting the wires with a silver paste-paint from Du Pont. The ends of the crystals were completely covered to provide uniform current flux. The sample mounting allowed the crystal to expand and contract as a consequence of thermal cycles.

The dc measurements were carried out by applying a stabilized current of about 1 μA for all temperatures investigated. The temperature was stabilized and measured with an accuracy of about 0.5 deg. For the absolute conductivity values the thickness, width, and length of the crystal between the potential contacts were measured by using a reticule and microscope. The error introduced by the uncertainty of the sample dimensions was of the order of 10%.

The thermoelectric power of the crystal was measured by the method of alternating temperature gradient. The maximum temperature drop across the sample was less than 0.5 deg. From room-temperature to about 100 K, the temperature was lowered at a rate of 1 deg min^{-1} in both the Seebeck coefficient and dc conductivity measurements.

Spectral investigations of the TCNQ salts with metallocene derivatives were performed in the intermediate-IR region (between 4000 and 400

- (1) Shchegolev, I. F. *Phys. Status Solidi A* **1972**, *12*, 9.
- (2) André, J.-J.; Bieber, A.; Gautier, F. *Ann. Phys.* **1976**, *1*, 145.
- (3) Keller, H. J., Ed. *Low Dimensional Co-operative Phenomena*; Plenum: New York, 1975.
- (4) Keller, H. J., Ed. *Chemistry and Physics of One-Dimensional Metals*; Plenum: New York, 1977.
- (5) Keller, H. J., Ed. *Extended Linear Chain Compounds*; Plenum: New York, 1982, 1983; Vols. 1-3.
- (6) Lequan, R.-M.; Lequan, M.; Jaouen, G.; Ouahab, L.; Batail, P.; Padiou, J.; Sutherland, R. G. *J. Chem. Soc., Chem. Commun.* **1985**, 116.
- (7) Willi, C.; Reis, A. H., Jr.; Gebert, E.; Miller, J. S. *Inorg. Chem.* **1981**, *20*, 313. Lemenovskii, D. A.; Urazovskii, I. F.; Baukova, T. V.; Arkhipov, I. L.; Stukan, R. A.; Perevalova, E. G. *J. Organomet. Chem.* **1984**, *264*, 283. Isima, S.; Tanaka, Y. *J. Organomet. Chem.* **1984**, *270*, C11.

[†] Permanent address: Institute of Physics, Agricultural Academy, Poznań, Poland.

^{††} Polish Academy of Sciences.

[§] CNRS.

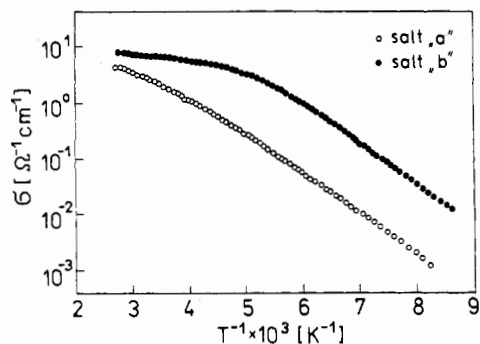


Figure 1. Electrical conductivity σ for typical samples of salts a and b.

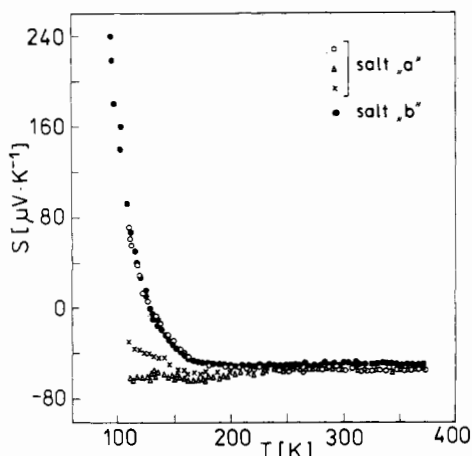


Figure 2. Seebeck coefficient S for typical samples of salts a and b. The strong sample dependence of S for the former is seen below about 200 K.

cm^{-1}) by using a SPECORD M 80 spectrophotometer with a variable-temperature attachment. The samples were prepared by compressing the finely powdered salts with KBr, at a weight ratio of 1:1000. The range of the temperature measurements was from room temperature to about 100 K with temperature stabilization better than 0.5 deg.

Results

1. Salt a: $[(\text{cp})\text{Fe}^{\text{II}}(2,4,6\text{-C}_6\text{H}_3\text{Me}_3)]^+(\text{TCNQ})_2^-$. The temperature characteristics of dc conductivity, $\sigma(T)$, were measured for about ten samples. The data for a typical single-crystal sample are shown in Figure 1. The absolute values of the room-temperature conductivity observed for the needle axes of the crystals were between 2.75 and $7.9 \Omega^{-1} \text{cm}^{-1}$, resulting in an average value of $\sigma(300) = 5.3 \Omega^{-1} \text{cm}^{-1}$.

$\sigma(T)$ exhibits semiconducting-like behavior with a constant activation energy, $E_a = 0.15 \text{ eV}$, up to the limit temperature T_d . Temperature T_d is also sample-dependent, and for extreme cases it falls between 200 and 160 K.

The Seebeck coefficient S , describing the thermoelectric properties of the salt, is presented in Figure 2. The S coefficient exhibits temperature-independent behavior over a wide temperature range from about 200 to 370 K. For different samples, S lies between -54 and $-66 \mu\text{V K}^{-1}$, but most of the crystals exhibited a value of $-58 \mu\text{V K}^{-1}$. Below about 200 K, $S(T)$ is strongly sample-dependent; two extreme examples and an intermediate example are shown in Figure 2 also.

The IR spectrum of salt a is dominated by a very large CT band at about 3300 cm^{-1} and a set of bands resulting from a vibronic activation of the a_g modes of TCNQ by delocalized electrons. These bands are seen at 606, 698, 953, 1132, 1328, 1560, and about 2170 cm^{-1} , at 297 K. They are due to the vibronic activation of totally symmetric (a_g) ν_8 to ν_2 modes of TCNQ, respectively. The temperature shifts of these bands are rather small and are detectable only for some; e.g., ν_4 shifts from 1328 to 1331 cm^{-1} at 81 K. From the comparison of the low-temperature (81 K) spectrum and that at 297 K, it is evident that the intensity of the vibronically activated bands is remarkably enhanced in the low-

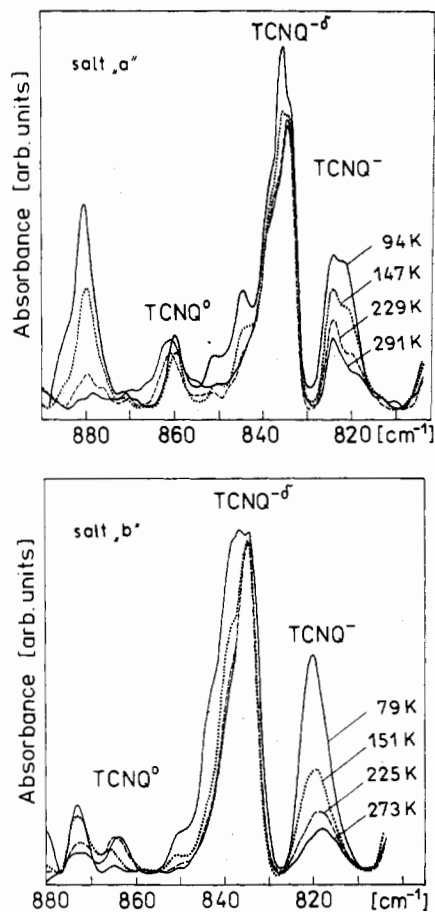


Figure 3. Evolution of the IR spectra of (a) salt a and (b) salt b in a KBr pellet. Attribution of the bands to out-of-plane u modes of the TCNQ^0 molecule, the $\text{TCNQ}^{\cdot-}$ radical, and the $\text{TCNQ}^{\cdot-}$ ion with a fractional charge is given.

temperature phase. The temperature dependences of these intensities are smooth and do not display any anomalies.

The frequencies of vibrational out-of-plane u modes of TCNQ depend on the degree of charge transfer between the two TCNQ species, and the frequency shift of some of them can be large.^{8,9} We used this modification of the out-of-plane vibrational frequency as an indicator of the electron localization. The IR spectrum of salt a is shown in Figure 3a. The pair of bands at 862 and 820 cm^{-1} is most suitable for these observations. Their thermal evolution will be discussed later, together with the evolution of the appropriate bands of salt b.

2. Salt b: $[(\text{cp})\text{Fe}^{\text{II}}(\text{C}_6\text{Me}_6)]^+(\text{TCNQ})_2^-$. Measuring the thermal variation of dc conductivity, $\sigma(T)$, we noticed random, irreversible drops of σ , even of 1 order of magnitude. Detailed examination of the crystal surfaces under a polarized microscope with $500\times$ magnification did not show any cracks or surface changes. Probably the internal microcracks of the samples are the reason of the observed drops of $\sigma(T)$.

The typical thermal variation of the $\sigma(T)$ of salt b is shown in Figure 1. The average conductivity value at 300 K is $6.6 \pm 0.8 \Omega^{-1} \text{cm}^{-1}$; $\sigma(T)$ exhibits activative character with $E_a = 0.15 \text{ eV}$ at low temperatures, up to approximately 170 K. Similar to that of the preceding salt, the Seebeck coefficient of salt b is temperature-independent at high temperatures, above about 170 K (Figure 2). Its average value in this temperature range is $-52 \mu\text{V K}^{-1}$. Below 170 K the thermoelectric power increases, crossing $0 \mu\text{V K}^{-1}$ near the temperatures 125–130 K.

The IR spectrum of salt b resembles the spectrum of salt a and other conducting TCNQ salts. The activated a_g modes dominate

(8) Bozio, R.; Zanon, I.; Girlando, A.; Pecile, C. *J. Chem. Soc., Faraday Trans. 2* 1978, 74, 235.

(9) Farges, J. P.; Brau, A.; Dupuis, P. *Solid State Commun.* 1985, 54, 531.

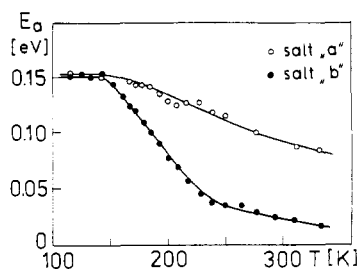


Figure 4. Activation energy E_a for typical samples of salts a and b.

over the spectrum. The temperature dependences of these vibrationally activated bands are also smooth. An analysis of the thermal evolution of the spectrum between 800 and 880 cm^{-1} (Figure 3b) yields valuable information. At room temperature, the spectrum is well resolved and consists of four bands at 874, 864, 835, and 819 cm^{-1} . The two peaks at 864 and 819 cm^{-1} are well identified, being associated with a vibrational out-of-plane u mode of the TCNQ^0 molecule and TCNQ^- radical, respectively.⁸ Only the first one is observed in the spectrum of the fully neutral sample, and only the second one, in the spectrum of the fully ionized salt. The third peak, with an intermediate frequency (835 cm^{-1}), has no equivalent in the spectra of either the fully neutral or fully ionized samples. It can be viewed as the corresponding feature for TCNQ molecules with only a fractional charge. According to Farges et al.⁹ it is most probably the signature of the delocalized electrons in the salt and, in particular, of the anionic species $(\text{TCNQ})_{2^-}$. The left peak, at 874 cm^{-1} , is considered as a combination vibration of TCNQ molecule.

Although the general appearance of the spectrum between 800 and 880 cm^{-1} is maintained at low temperature (Figure 3), relative intensities of the bands, and even the shape of the peaks, change characteristically with temperature.

Discussion

Significant analogies can be found in the transport and spectral properties of the two TCNQ salts with metallocene ions. Comparing the temperature dependences of $\sigma(T)$ (Figure 1) as well as $S(T)$ (Figure 2), one may state that the mechanism of the electrical transport is the same in the two salts. In the low-temperature region the conductivity shows activative character with well-defined activation energy $E_a = 0.15$ eV, for both salts. The weaker T dependence of $\sigma(T)$ at higher temperature shows that the dc conductivity of the salts cannot be explained in terms of the band model of a semiconductor with a constant energy gap and weak T dependence on the mobility of charge carriers. Even in the presence of various impurity states inside the gap, the activation energy should be increasing with temperature, contrary to the experimental evidence.

The character of T dependence of $\sigma(T)$ and the rather high values of the conductivity at room temperature $\sigma(300)$, as well as the spectral features proving the strong electron-phonon coupling, would suggest the Epstein-Conwell model¹⁰ with a large, strongly T -dependent mobility determined mainly by the interaction with molecular vibrations. However, the linear and the nonlinear regions of the T dependence of the conductivity could not simultaneously be described with their formula. The Epstein-Conwell model had to be rejected in view of the failure to fit the experimental data points in any of the two regions. Similarly, the hopping models (e.g. diffusive hopping or variable-range phonon-assisted hopping) did not yield a correct description of $\sigma(T)$ for the two salts.

The observed thermopower value is close to the values found for a number of TCNQ salts with approximately one electron per two TCNQ molecules, on average.¹² This means that the Seebeck

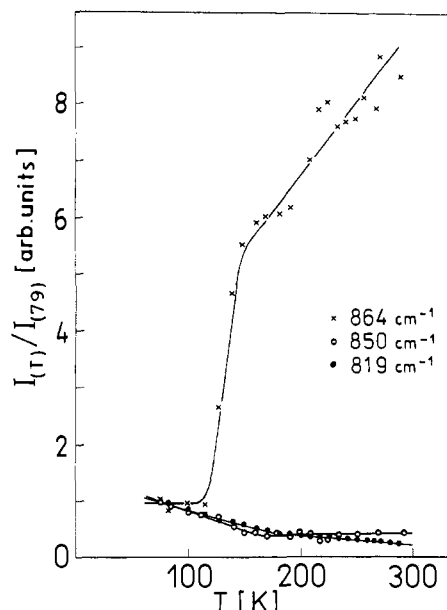


Figure 5. Normalized integral intensities of the u modes of TCNQ^0 (864 cm^{-1}), TCNQ^- (819 cm^{-1}), and one $\text{TCNQ}^{0.5-}$ (850 cm^{-1}).

coefficient of the two salts can be described by the Chaikin and Beni model¹³ of correlated electrons with strong Coulomb interactions; this model leads to $S = -60 \mu\text{V K}^{-1}$, for $\rho = 0.5$ at high temperature. The sample-dependent S for a salt may be caused by defects giving rise to additional contributions, apart from the statistical one.¹⁴

Analysis of the function $d \ln \sigma(T)/d(1/T)$ gives the T dependence of the activation energy E_a or the gap $E_g = 2E_a$; $E_a(T)$ curves for both salts are shown in Figure 4.

Only at low temperature is E_a constant, amounting to 0.15 eV irrespective of the salt and sample. T dependence of E_a was observed above 150 K for salt a and above about 140 K for salt b. At high temperature, above about 230 K (salt b), the T dependence of E_a becomes weaker, and the value of E_a approaches 0.015 eV. This peculiarity of the gap reflects the electronic structure of the TCNQ chain.

According to the structure data⁶ of salt b, a quarter-filled band describes the TCNQ chain at high temperature; this is not the situation occurring in insulators. In order to explain the semi-conducting character of the salts, we need either a strong tetramerization or a substantial Coulomb interaction to keep the electrons apart.

It follows from Figure 3 that the band at 835 cm^{-1} becomes asymmetric and splits at low temperature into four components: 835, 840, 844, and 850 cm^{-1} . Assuming that the frequency shift $\Delta\nu = \nu(\text{TCNQ}^0) - \nu(\text{TCNQ}^-)$ is proportional to the charge δ on the partly charged $\text{TCNQ}^{0.5-}$ ion,¹¹ we assign these lines to out-of-plane vibrations of $\text{TCNQ}^{0.5-}$ with $0.3 < \delta < 0.6$. It appears that this splitting shows the existence of four nonequivalent $\text{TCNQ}^{0.5-}$ ions. The T dependences of the normalized integral intensities of u modes of TCNQ^0 (864 cm^{-1}), TCNQ^- (819 cm^{-1}), and one $\text{TCNQ}^{0.5-}$ (850 cm^{-1}) are shown in Figure 5.

From the analysis of Figures 3 and 5 and the T dependence of the intensities of the remaining bands, we can ascertain that the TCNQ chain at high temperature (about 297 K) is structured mainly with $\text{TCNQ}^{0.5-}$ ions with δ about 0.5. The content of TCNQ^0 and TCNQ^- is about 10 times smaller. At low temperature (about 80 K) the $\text{TCNQ}^{0.5-}$ ion dominates although appreciable amounts of TCNQ^- and $\text{TCNQ}^{0.5-}$ ions with $\delta < 0.5$ are observed. The content of TCNQ^0 molecules approaches zero on lowering the temperature. The appearance of the different, but well-defined, TCNQ species points to localization of the

(10) Epstein, A. J.; Conwell, E. M.; Miller, J. S. *Ann. N.Y. Acad. Sci.* **1978**, *313*, 183.

(11) Matsuzaki, S.; Kuwata, R.; Toyoda, K. *Solid State Commun.* **1980**, *33*, 403.

(12) Chaikin, P. M.; Kwak, J. F.; Epstein, A. J. *Phys. Rev. Lett.* **1979**, *42*, 1178.

(13) Chaikin, P. M.; Beni, G. *Phys. Rev. B: Solid State* **1976**, *13*, 647.

(14) Zuppiroli, L.; Przybylski, M.; Pukacki, W. *J. Phys. (Les Ulis, Fr.)* **1984**, *45*, 1925.

electrons and formation of nonregular TCNQ chains, probably tetramerized. Such tetramerization can be the result of a specific interaction between TCNQ and dipole moments of cations. In this situation a systematic temperature change in the activation energy, E_a , can occur.

Conclusions

TCNQ complex salts with metallocene ions represent an interesting class of semiconducting organometallic compounds. Their transport and spectral properties are determined by the appearance of TCNQ chains. At high temperature the chains are nearly uniform, with delocalized electrons. This delocalization is seen from both spectral and transport properties. At low temperature the salts are characterized by nonregular charge dis-

tribution along the chains. This is shown not only by the appearance of the energy gap at about 0.3 eV (and as a consequence the thermally activated electrical conductivity and strongly T dependent thermoelectric power) but also directly by the presence of the new absorption bands characteristic of TCNQ⁻ with $0.3 < \delta < 0.6$.

The physical properties of TCNQ salts with metallocene ions are not unusual for organic low-dimensional conductors. The large, three-dimensional ions do not cause significant changes in the properties of the salts. This points to a secondary role for the counterions in TCNQ salts. However, in order to achieve a definitive interpretation of the properties of the salts, it appears necessary to include studies of other phenomena, especially spin ordering, for which ESR measurements will soon be carried out.

Contribution from the Research School of Chemistry, Australian National University, Canberra, ACT 2601, Australia, Institut für anorganische Chemie, Universität Basel, Basel, Switzerland, and Department of Chemistry, University of Canterbury, Christchurch, New Zealand

Electronic and Molecular Structure of $[\text{Cr}(\text{bpy})_3]^{3+}$ (bpy = 2,2'-Bipyridine)

A. Hauser,*† M. Mäder,‡ W. T. Robinson,§ R. Murugesan,† and J. Ferguson†

Received October 7, 1986

$[\text{Cr}(\text{bpy})_3](\text{PF}_6)_3$ and $[\text{Rh}(\text{bpy})_3](\text{PF}_6)_3$ both crystallize in the trigonal space group $R\bar{3}2$, with site symmetry D_3 for the metal ions. Absorption and Zeeman spectra of neat $[\text{Cr}(\text{bpy})_3](\text{PF}_6)_3$ and dilute $[\text{Rh}(\text{bpy})_3](\text{PF}_6)_3:\text{Cr}^{3+}$ in the region of ligand field transitions as well as emission spectra and EPR of the latter have been studied. Ground-state (4A_2) and first-excited-state (2E) zero-field splittings and g values for Cr^{3+} and assignments of bands at higher energy to $^4A_2 \rightarrow ^2T_1$ electronic origins are reported. The fine structure in the region of the $^4A_2 \rightarrow ^4T_2$ and 2T_2 transitions is ascribed to vibrational sidebands of the former.

1. Introduction

Cr^{3+} coordination compounds have received a lot of attention over the last two decades. The initial papers by Sugano et al.^{1,2} on the electronic structure of the 4A_2 ground state and the 2E , 2T_1 , and 2T_2 excited states in a trigonally distorted ligand field (LF) gave the incentive for a lot of experimental and theoretical work²⁻⁴ mainly on Cr^{3+} doped into crystal lattices containing oxygen as the coordinating ligand, such as ruby, emerald, spinels, and garnets. For these compounds it has generally been possible to account for the low-lying metal-centered energy levels, and their zero-field splittings and g values, by diagonalizing the full d^3 LF matrix, including an axial component along the trigonal axis and an external magnetic field together with the octahedral LF, the electrostatic interaction, and spin-orbit coupling.⁵ The inclusion of the two trigonal LF parameters K and K' (as defined by Sugano and Tanabe¹) in the calculation was particularly successful in rationalizing the zero-field splitting of the 4A_2 ground state, the zero-field splittings of the 2E , 2T_1 , and 2T_2 excited states, and the g values of the 2E components. All of these quantities depend largely on K and K' and to some extent on the spin-orbit coupling constant ζ and are more or less independent of the Racah parameters B and C and the octahedral part of the LF $10Dq$, which basically determine the absolute energy of the various energy levels but not their splittings.

Cr^{3+} coordination compounds with nitrogen-containing ligands have been studied over the last few years in quite a different context. It was and still is their photoactivity that makes them attractive.⁶ Most investigations of nitrogen-coordinated Cr^{3+} compounds have therefore centered around their photochemistry, observed mainly in solution and glasses,⁷ and the elucidation of the electronic structure has been somewhat neglected. Solomon et al.⁸ have performed an analysis of the $^4A_2 \rightarrow ^4T_2$ d-d transition in $[\text{Cr}(\text{NH}_3)_6](\text{ClO}_4)_2\text{Cl}\cdot\text{KCl}$ on the basis of a dynamic Jahn-

Teller effect, and Güdel et al.,⁹ McCarthy and Vala,¹⁰ and Geiser and Güdel¹¹ have done some optical measurements on $2[\text{Cr}(\text{en})_3]\text{Cl}_3\cdot\text{KCl}\cdot 6\text{H}_2\text{O}$.

However, in order to come to grips with the photochemical behavior of nitrogen-coordinated Cr^{3+} compounds, it seems to us to be of prime importance to know what the electronic structure of a given species is, paying special attention to its molecular symmetry. This prompted us to study $[\text{Cr}(\text{bpy})_3]^{3+}$ (bpy = 2,2'-bipyridine) both as the pure PF_6^- salt and in a dilute form, doped into isostructural $[\text{Rh}(\text{bpy})_3](\text{PF}_6)_3$. The advantage of these compounds is that the inherent molecular symmetry of the $[\text{Cr}(\text{bpy})_3]^{3+}$, namely D_3 , is retained in the crystal lattice.

In this paper the single-crystal X-ray structures of both $[\text{Cr}(\text{bpy})_3](\text{PF}_6)_3$ and $[\text{Rh}(\text{bpy})_3](\text{PF}_6)_3$, single-crystal and powder EPR spectra of $[\text{Rh}(\text{bpy})_3](\text{PF}_6)_3:\text{Cr}^{3+}$, and the low-temperature absorption spectra of both the neat and the dilute material in the region of d-d transitions as well as the low-temperature emission spectrum of the dilute material are reported. A full d^3 LF calculation, including the electrostatic interaction, the octahedral and trigonal parts of the LF, spin-orbit coupling, and an external magnetic field, was carried out in order to interpret the experimental results quantitatively.

2. Experimental Section

Synthesis and Crystal Growth. $[\text{Rh}(\text{bpy})_3](\text{PF}_6)_3$.¹² A 0.5-g sample

- (1) Sugano, S.; Tanabe, Y. *J. Phys. Soc. Jpn.* **1958**, *13*, 880.
- (2) Sugano, S.; Tsujikawa, J. *J. Phys. Soc. Jpn.* **1958**, *13*, 899.
- (3) McFarlane, R. M. *J. Chem. Phys.* **1962**, *39*, 3118.
- (4) McFarlane, R. M. *Phys. Rev. B: Solid State* **1970**, *1*, 989.
- (5) McFarlane, R. M. *J. Chem. Phys.* **1967**, *47*, 2066.
- (6) Endicott, J. F. *J. Chem. Educ.* **1983**, *60*, 824.
- (7) Allsop, S. R.; Cox, A.; Kemp, T. J.; Reed, W. J. *J. Chem. Soc., Faraday Trans. 1* **1980**, *76*, 162.
- (8) Wilson, R. B.; Solomon, E. I. *Inorg. Chem.* **1978**, *17*, 1729.
- (9) Güdel, G. U.; Trabjerg, I. B.; Vala, M.; Ballhausen, C. J. *Mol. Phys.* **1972**, *24*, 1227.
- (10) McCarthy, P. J.; Vala, M. *Mol. Phys.* **1973**, *25*, 17.
- (11) Geiser, U.; Güdel, H. U. *Inorg. Chem.* **1981**, *20*, 3013.
- (12) Harris, C. M.; McKenzie, E. D. *J. Inorg. Nucl. Chem.* **1963**, *25*, 171.

* Australian National University.

† Universität Basel.

‡ University of Canterbury.